Sustainability in Mechanical and Materials Design

smmd.pol-aca.com

Article

Numerical Study on the Failure Behavior of Metal Matrix Composites Based on a Coupled Phase Field-Cohesive Zone Model

Tao Gu [1*] ,Haodong Yang [2], Le Liang[3] , Wenzhuo Li [4]

[1]Guizhou Aerospace Fenghua Precision Equipment Co.Ltd, GuiYang,Guizhou, China.
[2]Kaili University, School of Mechanical Engineering, Kaili,Guizhou, China.
[3]Chongqing University of Technology,School of Mechanical Engineering, Chongqing,China.
[4]Southwest Forestry University,School of Mechanical Engineering,Kunming,Yunnan,China

ARTICLE INFO

Keywords:
Metal matrix composites
Phase field method
Cohesive zone model
Strain rate effect
Temperature effect

ABSTRACT

This paper employs a coupled ductile phase field fracture model (PFM) and cohesive zone model (CZM) to numerically investigate the failure behavior of a representative volume element (RVE) of a Ti-6Al-4V metal matrix composite containing SiC particles. By systematically analyzing the influence of factors such as mesh size, interfacial fracture parameters, particle distribution, volume fraction, strain rate, and temperature on the mechanical response and crack propagation, the complete failure mechanism from interface debonding to matrix crack is revealed. The results indicate that the mesh size significantly affects the sensitivity of matrix damage simulation, while interfacial strength and fracture energy markedly influence the overall mechanical performance of the composite. Variations in particle distribution and volume fraction lead to differences in crack paths and ductile behavior. Changes in strain rate and temperature cause a transition in the failure mode from interface-dominated to matrix-dominated. This study provides a theoretical basis and numerical tools for the multi-scale failure analysis and structural optimization of metal matrix composites.

1. Introduction

Metal matrix composites (MMCs) are widely used in aerospace, automotive industries, and defense sectors due to their high specific strength, good high-temperature performance, and excellent wear resistance. However, due to their multi-phase structure and complex interfacial behavior, the failure mechanisms of composites involve the coupling of multiple physical processes such as interface debonding, matrix plastic deformation, and crack propagation. Traditional

* **Correspondence authors**

Email address:709122278@qq.com

Citation: To be added by editorial staff during production.

macroscopic phenomenological models struggle to accurately describe their mesoscopic failure behavior. Therefore, developing numerical models capable of characterizing the continuous damage process from the interface to the matrix is of great significance

2. Literature Review

In recent years, the coupled use of the phase field fracture model (PFM) and the cohesive zone model (CZM) has become an effective means for simulating composite failure. PFM is suitable for simulating diffuse crack propagation, while CZM excels at describing interface separation behavior. This paper combines both to study the failure process of Ti-6Al-4V/SiC composites, systematically exploring the influence of various factors on their mechanical behavior.

Research on the failure mechanisms of metal matrix composites (MMCs) began in the 1980s, with early work primarily focused on experimental observation and the establishment of macroscopic phenomenological models. Since the 1990s, with the development of computational mechanics, numerical simulation has gradually become an important tool for studying the mesoscopic failure behavior of composites. From the 1990s to the early 2000s, most studies used homogenization models based on Eshelby's inclusion theory or the Mori-Tanaka method, treating the composite as an equivalent homogeneous medium to predict macroscopic elastic modulus and strength (Nemat-Nasser & Hori, 1993). Although computationally efficient and suitable for preliminary material design, such methods cannot capture local failure behaviors, such as interface debonding, particle fracture, and matrix crack propagation.

To address this limitation, researchers began introducing interface elements to simulate the interface failure process. The cohesive zone model (CZM) proposed by Needleman (1987) became a key tool for simulating interface debond, describing the nonlinear fracture behavior of interfaces through a traction-separation law. However, CZM is inherently phenomenological and struggles to couple with matrix plastic deformation and damage evolution, particularly in describing the dynamic propagation of cracks in high-toughness metal matrices (Tvergaard & Hutchinson, 1992). Subsequently, multi-scale modeling methods gradually emerged, with the representative volume element (RVE) becoming a key bridge connecting microstructure and macroscopic properties. Ghosh et al. (1995) first combined RVE with the finite element method to successfully predict the elasto-plastic response of composites; Vaughan and McCarthy (2011) further introduced RVE to simulate damage initiation in particle-reinforced composites, but their model still relied on predefined failure criteria and could not naturally describe crack initiation and propagation paths.

Since 2010, with the rise of the phase field method (PFM), significant progress has been made in simulating composite fracture. PFM avoids the difficulty of explicitly tracking crack geometry by introducing a diffuse crack representation, making it suitable for simulating complex crack paths (Miehe et al., 2010). Borden et al. (2014) extended it to elasto-plastic materials, enhancing the model's ability to describe ductile fracture. However, pure phase field models still have limitations in handling interface behavior, particularly in accurately reflecting the failure competition mechanism between the interface and the matrix. In recent years, models coupling CZM and PFM have gradually become a research focus. For example, Li et al. (2019) used a coupled method to simulate interface debonding and matrix cracking in composites, but the predicted crack propagation paths still showed some deviation from experimental results. Zhang et al. (2021) pointed out that the

strain energy decomposition method is an important factor causing simulation differences, as different decomposition forms significantly affect crack deflection behavior and the final failure mode.

Although coupled models are theoretically advantageous, most current studies still have three main limitations: firstly, high computational cost and poor convergence make them difficult to apply to large multi-particle systems; secondly, most models do not fully consider strain rate and temperature effects, limiting their predictive capability in thermo-mechanically coupled fields; thirdly, the randomness of particle morphology, distribution, and interface properties is often simplified, reducing the model's generalizability and engineering applicability.

Within this research context, this paper adopts a non-coupled CZM-PFM modeling strategy, separately handling interface and matrix failure, ensuring numerical stability while maintaining physical realism. By introducing strain rate- and temperature-dependent interfacial constitutive relations, the failure behavior of composites under multi-field coupling environments is systematically studied to mitigate the shortcomings of existing models in simulating dynamic and thermodynamic behavior, providing a reliable numerical tool for the design of high-performance composites.

3. Research Methods and Conclusions

3.1 Numerical Simulation of Single-Particle RVE

3.1.1 Influence of Mesh Size

Due to the complexity of the mechanical behavior of metal matrix composites, mesostructures with certain characteristics are usually selected based on the distribution of the composite to characterize the material's mechanical response. This mesostructure is called the representative volume element (RVE). Generally, the size of the composite RVE needs to be at least an order of magnitude larger than the particle size. This chapter considers the quasi-static tensile test of an RVE containing a single particle. The length of the single-particle RVE is selected as L = 10 mm, and the thickness is 0.25 mm. As ductile PFM and CZM need to be combined for modeling, a brief discussion on mesh size is first conducted to determine an appropriate mesh size. Three different mesh sizes are selected: 0.1 mm, 0.075 mm, and 0.05 mm. The length scale parameter is set to l_0 = 0.2 mm for all cases. Additionally, the applied displacement is 1.0 mm. The material parameters for the matrix Ti-6Al-4V are shown in Tables 1 and 2, with a fracture energy of G_f = 50 N/mm.

Table 1 Materials property of Ti-6Al-4V

Young's modulus, E / GPa	Possion's ratio, v	Density, ρ / kg·m^{-3}	Melting point, T_m / K	Specific heat c_T / J·(kg·K)$^{-1}$	Thermal conductivity, k_c / W·(m·K)$^{-1}$
109	0.34	4430	1878	611	6.8
A_{JC} / MPa	B_{JC} / MPa	C_{JC}	n_{JC}	m_{JC}	α_T / K^{-1}
891.5	630.3	0.034	0.547	0.9432	8.8×10^{-6}

Table 2 J-C damage parameters of Ti-6Al-4V

Parameters	D_1	D_2	D_3	D_4	D_5
Ti6Al4V	0.01546	1.349	−2.144	0.04323	0.6815

In the phase field model, the following equation is used to compute the plastic work threshold.

$$\varepsilon_{\mathrm{f}}=\left(D_1+D_2\exp\left(D_3\frac{\sigma_{\mathrm{hyd}}}{\sigma_{\mathrm{eq}}}\right)\right)\left[1+D_4\ln\left(\frac{\dot{\bar{\varepsilon}}_{\mathrm{p}}}{\dot{\varepsilon}_{\mathrm{ref}}}\right)\right]\left[1-D_5\left(\frac{T-T_{\mathrm{ref}}}{T_{\mathrm{m}}-T_{\mathrm{ref}}}\right)\right] \tag{1}$$

Where ε_{f} is the failure strain, σ_{hyd} is the hydrostatic pressure; D_1, D_2, D_3, D_4, and D_5 are material parameters, the values of which are listed in Table 2

The SiC particle is assumed to be purely elastic with an elastic modulus of 420 GPa, Poisson's ratio of 0.17, and density of 3150 kg/m³. Other parameters for the interface in the simulation are shown in Table 3.

Table 3 Parameters of cohesive elements

cohesive element	Value
Density, ρ/ kg·m^{-3}	4430
Fracture energy, $(G_{\mathrm{nc,tc,sc}})_{\mathrm{ref}}$ / N·mm^{-1}	30
Interface strength, $\overline{t}^{0}_{\mathrm{n,t,s}}$ /MPa	1000
Interface stiffness, $K_{\mathrm{n,s,t}}$ / N·mm^{-3}	1×10^{6}
Bond thermal conductivity, h_{bond} / W·(m·K)$^{-1}$	45
Contact thermal conductivity, h_{contact} / W·(m·K)$^{-1}$	100
Air thermal conductivity, h_{air} / W·(m·K)$^{-1}$	2

Note that the interfacial fracture energy here is taken as 15 N/mm, and the rate- and temperature-dependent parameters are $\zeta_1 = 0.0$, $\zeta_2 = 0.0$, $\kappa_T = 0.0$, $\varsigma_T = 0.0$. Other material parameters remain unchanged. The structural dimensions, boundary conditions, and the effect of mesh size are shown in Figure 1.

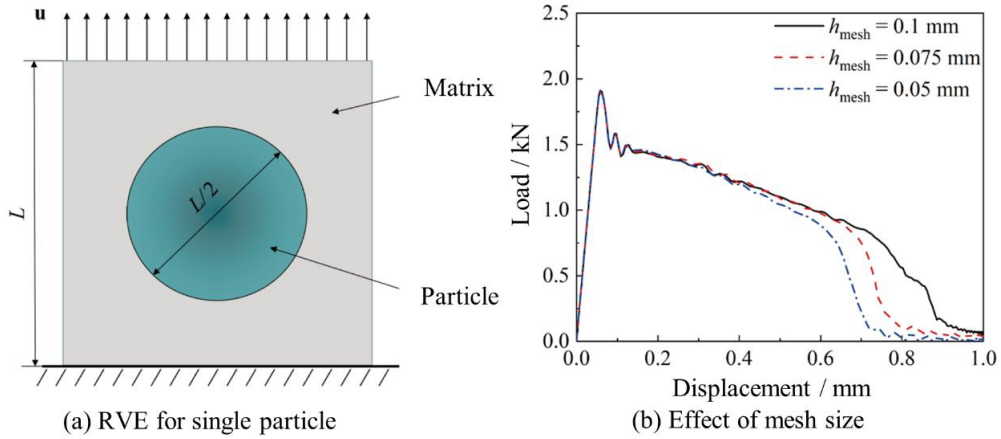

(a) RVE for single particle (b) Effect of mesh size

Figure 1 Effect of mesh size on single-particle RVE

From Figure1(b), it can be seen that the influence of mesh size on interface behavior is almost negligible, while its effect on ductile behavior is more significant. As the mesh size decreases, the failure displacement also decreases, reflecting the high sensitivity of the ductile PFM to mesh size. Larger mesh sizes result in larger crack length scales and wider diffuse crack bands, which is disadvantageous for characterizing crack propagation behavior in composites containing multiple particles. Therefore, a mesh size of 0.05 mm was ultimately selected for the numerical simulations in this paper.

3.1.2 Influence of Interfacial Fracture Parameters on Failure Behavior

In the numerical simulation of composites, the interface is the region most prone to failure. Its interfacial fracture parameters are directly related to the overall mechanical performance of the composite. Therefore, exploring the influence of interfacial fracture parameters on failure behavior is of great importance. First, the quasi-static tensile test of a single-particle RVE is used as an example to verify the validity of the model in this chapter. Subsequently, different interfacial fracture parameters are further investigated. The numerical simulation results for the single-particle RVE are shown in Figure 2.

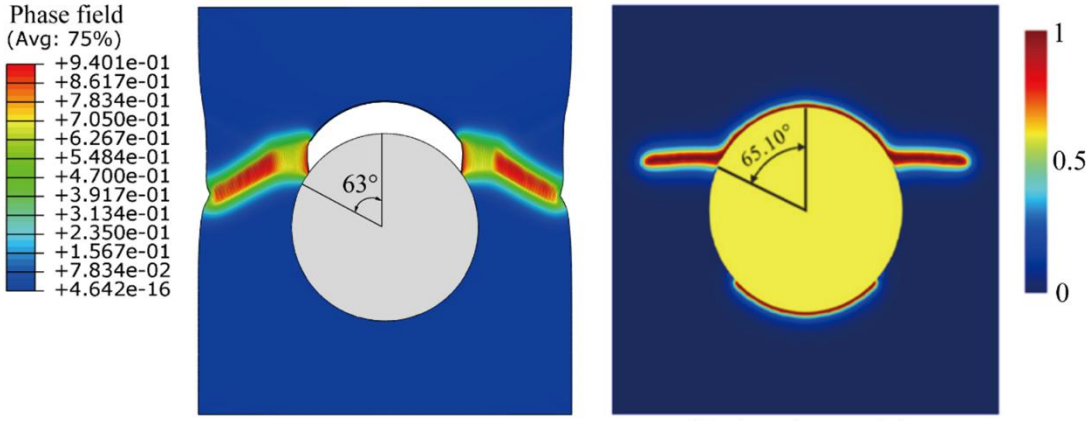

Figure 2 Comparison of crack propagation in single-particle numerical simulation (Elements are deleted when $d \geq 0.95$)

Figure 2 shows a comparison between the crack propagation direction in the single-particle RVE simulated by the current model and that in reference [227]. The results indicate that the angle between the crack nucleation location and the vertical direction is similar for both, i.e., 63° in this chapter versus 65.10° in the reference, both within a reasonable range (60°~70°) [228]. However, the crack propagation directions differ. The crack in this chapter propagates obliquely downward starting from the nucleation site, while the crack simulated by Li et al. [227] remains essentially horizontal. This difference primarily stems from the different strain energy decomposition methods used; a detailed analysis can be found in the work of Zhang et al. [228]. It is important to note that the two models combined in this chapter are non-coupled. When interface deboned occurs, the cohesive zone model takes effect. As the crack deflects into the matrix, the phase field fracture model controls the crack propagation. Furthermore, the crack propagation process in the single-particle numerical simulation is shown in Figure 3.

From Figure 3, it can be seen that the force-displacement curve of the single-particle RVE completely shows the entire process of crack propagation, which can be divided into four stages: ① Complete interface debonding; ② Crack initiation, matrix damage begins; ③ Crack gradually propagates; ④ Complete matrix failure. Specifically, as the loading

displacement increases, damage first begins to appear at the interface. When the loading displacement approaches 0.1 mm, the interface completely debond. As plastic deformation further increases and the equivalent plastic strain reaches the failure strain, the failure behavior transitions from interface debonding to matrix cracking. Subsequently, the matrix crack propagates obliquely downward at a certain angle to the vertical direction. Finally, when the loading displacement reaches 0.7 mm, the matrix completely cracks. In summary, the current model successfully captures the entire process from interface debond to matrix crack in the composite, providing a basis for subsequent research on multi-particle composites.

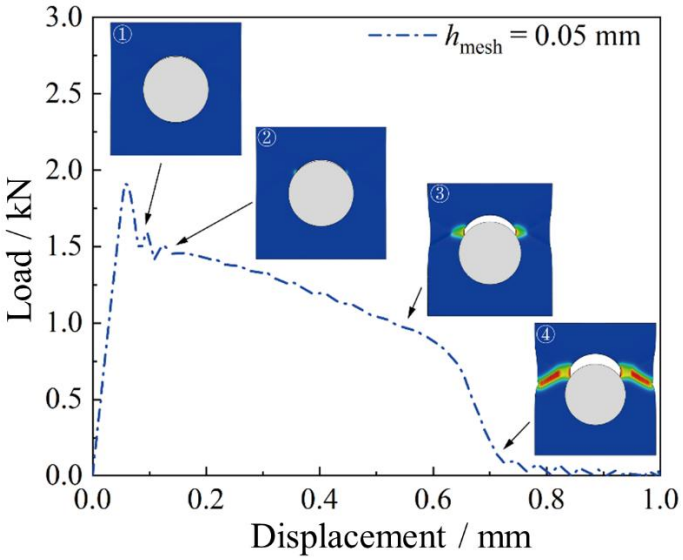

Figure 3 Force-displacement curve of the single-particle RVE

Interfacial fracture parameters mainly include interfacial strength and interfacial fracture energy, which determine the bonding strength between the matrix and particles. This chapter investigates the influence of interfacial strength $\bar{t}^0$ = 600, 841.9, 1100 MPa and interfacial fracture energy G_c = 15, 30, 45 N/mm on the mechanical response. The Load-displacement curves are shown in Figure 4.

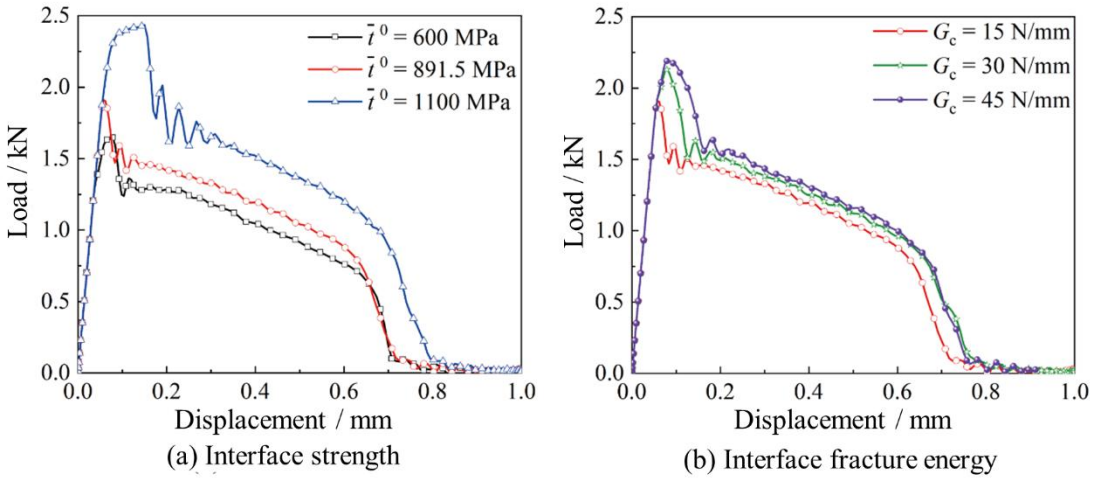

Figure 4 Influence of different interfacial fracture parameters on mechanical response

Figure 4(a) shows the influence of interfacial strength on the force-displacement curve at an interfacial fracture energy of G_c = 15 N/mm. The greater the interfacial strength, the higher the overall force-displacement curve of the metal matrix composite, indicating that stronger interfacial bonding is more conducive to improving the mechanical properties of the

composite. Figure 4(b) shows the influence of different interfacial fracture energies on the mechanical response at an interfacial strength of 891.5 MPa. It can be observed that a higher interfacial fracture energy leads to better mechanical performance of the composite and makes interface debonding less likely to occur, significantly enhancing the overall mechanical behavior of the composite. This implies that increasing the interfacial fracture energy can effectively improve the mechanical behavior of the composite. Additionally, crack propagation for different interfacial strengths and fracture energies is shown in Figure 5.

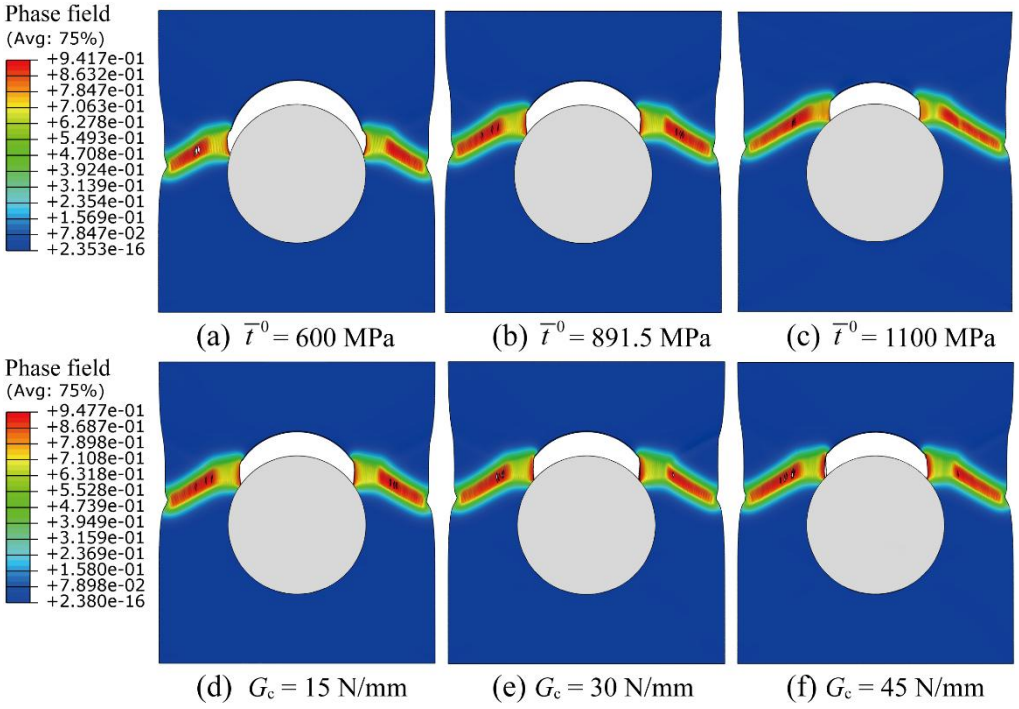

Figure 5 Crack propagation for different interfacial strengths and fracture energies

3.2 Numerical Simulation of Multi-Particle Composite RVE

Studying the mechanical behavior of composite RVEs containing multiple particles can reveal the complex processes of crack nucleation, growth, and coalescence, while further exploring the competition between interface debonding and matrix cracking, providing key insights for understanding the overall failure mechanism of composites.

3.2.1 Influence of Particle Distribution and Volume Fraction on Failure Behavior

This chapter generated RVEs containing different particle volume fractions using Python scripts, with a particle radius of 0.25 mm. As this chapter focuses on transverse mechanical behavior, the axial mechanical influence is not considered. Therefore, a thickness of 0.25 mm is selected to improve computational efficiency. Additionally, it is important to note that particle shape and size affect stress distribution, crack nucleation location, and crack propagation, thereby altering the overall mechanical properties of the composite. Compared to irregular particles, circular particles have a more uniform stress distribution, lower fracture tendency, and are more conducive to modeling. Thus, this chapter selects circular particles as the research object, generating different particle volume fractions of V_f = 10%, 20%, and 30%. The numerical models and boundary conditions are shown in Figure 6.

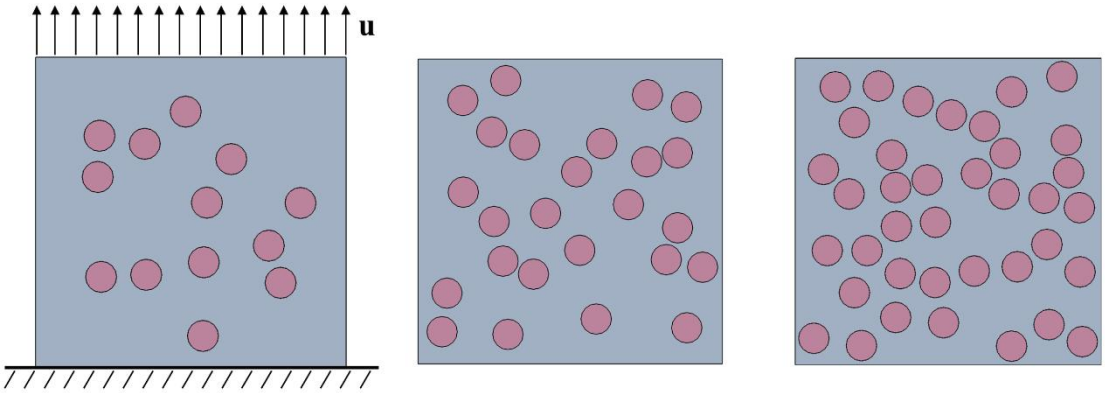

Figure 6 RVE with different particle volume fractions

On the other hand, quasi-static loading was applied to the multi-particle RVE. The material parameters for the matrix and particles are consistent with the previous subsection. Crack propagation for different particle distributions and volume fractions is shown in Figure 7.

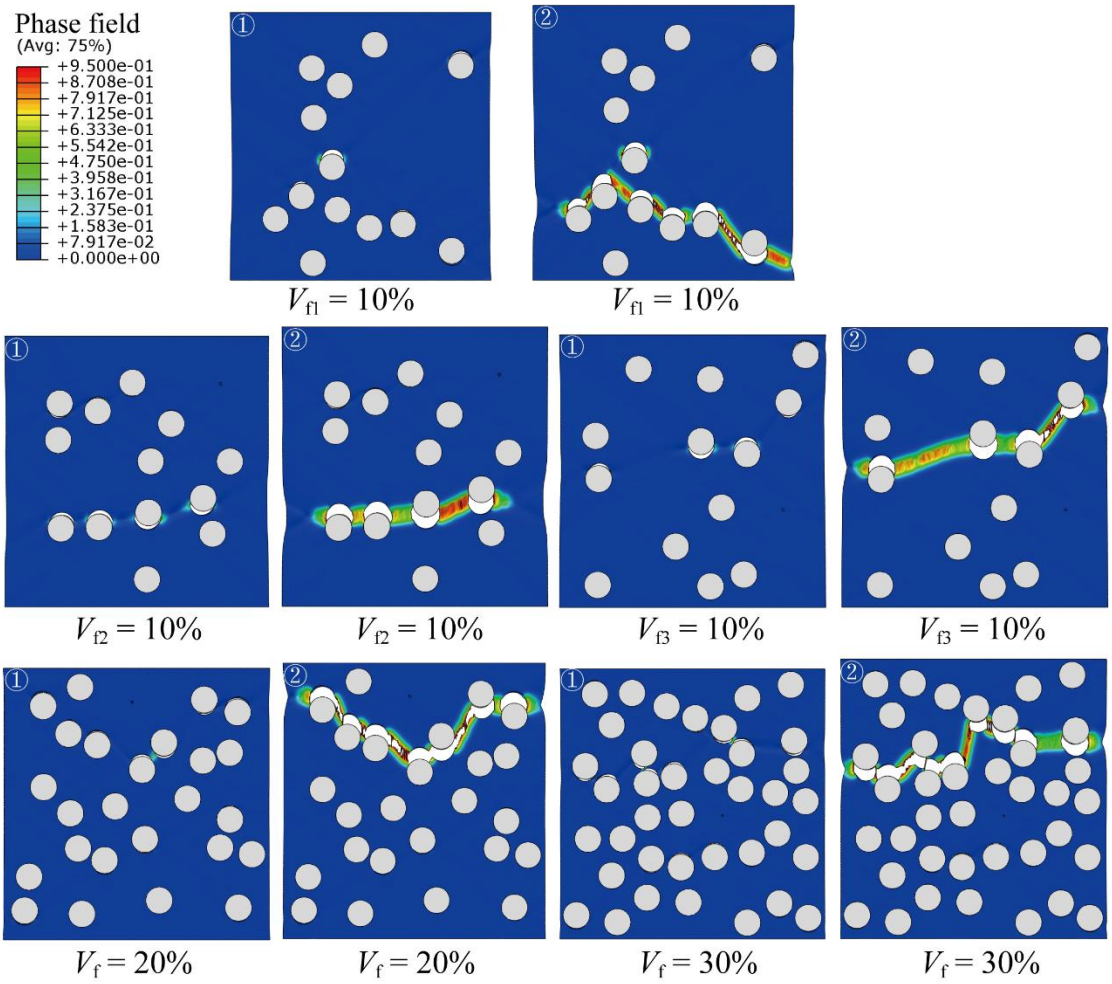

Figure 7 Crack propagation for different particle distributions and volume fractions

Figure 7 presents the process from crack initiation to failure for RVEs with different particle distributions and volume fractions. The results labeled ① in the figure represent the onset of matrix damage, while the symbol ② indicates the final fracture state of the material. From Figure 7, it can be generally observed that although the particle distributions (V_{f1}, V_{f2}, V_{f3}

= 10%) are different, crack initiation mostly occurs at the interface between the matrix and particles and gradually deflects into the matrix. As multiple interfaces debond, matrix cracks continuously connect to form crack paths. These phenomena indicate that the bonding strength between the matrix and particles is relatively low, causing the interface to debond first. Similarly, for RVE models with different particle volume fractions (V_f= 20%, V_f= 30%), the crack propagation process also exhibits similar behavior, except that the increase in particle volume fraction leads to more interface debonding and correspondingly more matrix damage. Through numerical simulation, the influence of particle distribution and volume fraction on crack propagation can be visually observed, aiding in the structural design and optimization of composites. In summary, the constructed damage model can effectively handle the entire process from brittle interfacial crack propagation to elasto-plastic matrix cracking. The force-displacement curves for different particle distributions and volume fractions are shown in Figure 8.

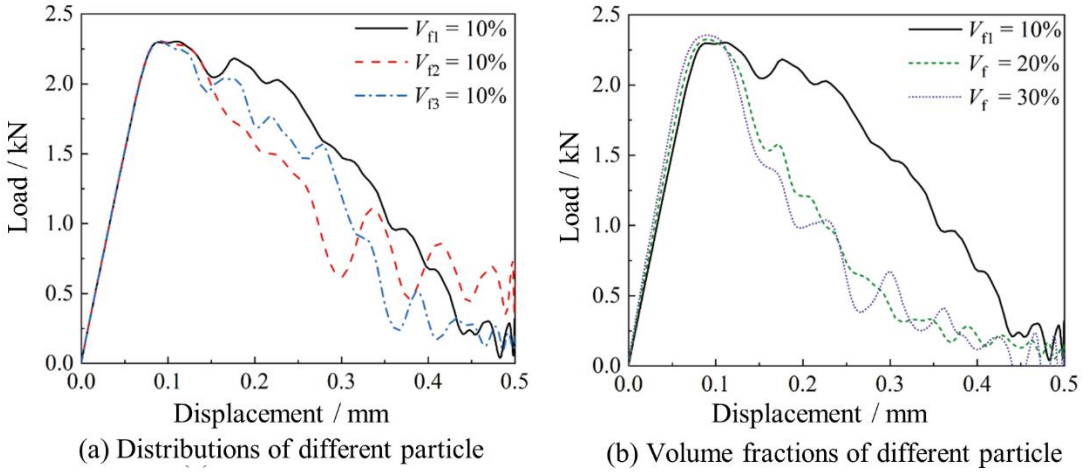

Figure 8 Load-displacement response for different particle distributions and volume fractions

From Figure 8, it can be seen that in the elasto-plastic stage, different particle distributions for a volume fraction of V_f = 10% show good consistency. The main differences are evident in the damage stage, and it can be observed that the ductile behavior of the V_{f1} = 10% particle distribution is better than the other two distributions. This also indicates that the local particle distribution at the same volume fraction has a certain influence on the overall mechanical response. However, the overall mechanical response is also affected by the particle volume fraction. As the particle volume fraction increases, the overall ductility of the composite decreases, making the material more brittle, but it increases the peak strength, allowing the material to withstand greater loads. Furthermore, it can be observed that an increase in particle volume fraction increases the elastic modulus of the RVE model. These phenomena indicate that reasonable particle distribution and volume fraction have a significant impact on the overall mechanical behavior of the composite and also reflect the ability of the model established to predict and capture these characteristics.

3.2.2 Influence of Strain Rate and Temperature on Failure Behavior

Based on the current model, using the RVE model with a particle volume fraction V_f = 30% as an example, the influence of strain rate and temperature on the mechanical behavior and crack propagation of the composite is explored. This analysis considers not only the strain rate and temperature sensitivity of the matrix material but also explores the effect of strain rate and temperature on interface failure, providing a more comprehensive understanding of the dynamic mechanical response of the composite at different temperatures. At room temperature (298 K), different loading velocities

were applied to the RVE model to explore the influence of strain rate on the mechanical behavior and crack propagation of the composite. Here, the rate- and temperature-dependent cohesive model parameters are $\zeta_1 = 0.02$, $\zeta_2 = 0.01$, $\kappa_T = 0.03$, $\varsigma_T = 0.01$. The reference interfacial fracture energy is 15 N/mm, and the reference interfacial strength is 891.4 MPa. The numerical simulation results are shown in Figure 9.

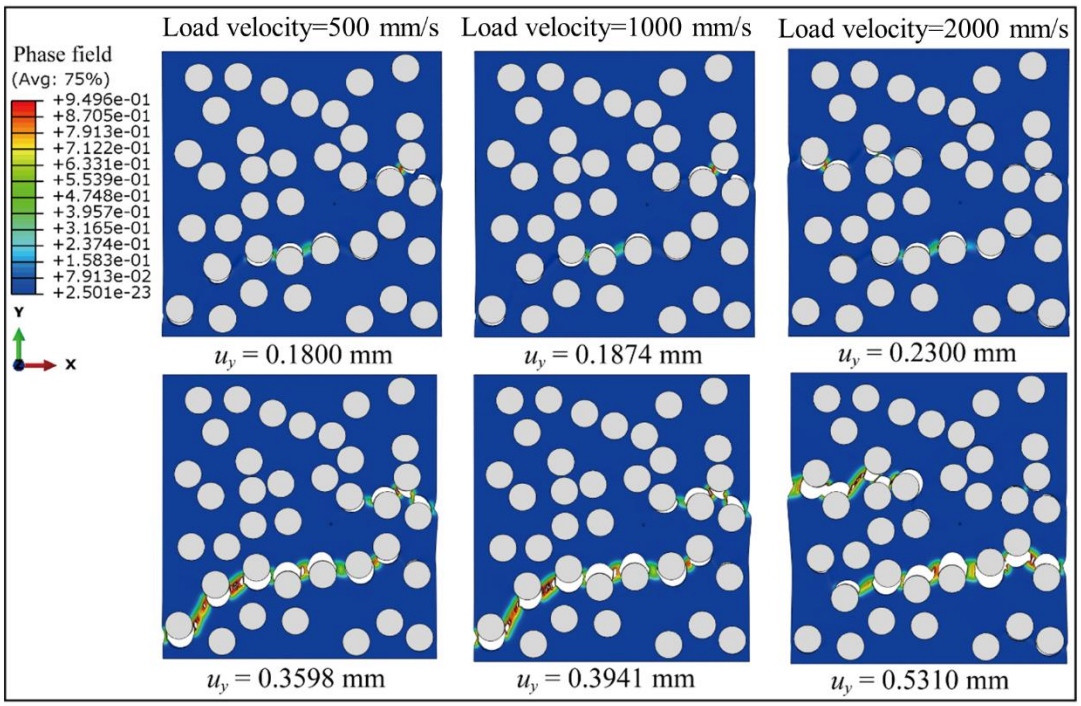

Figure 9 Crack propagation at different load velocities

From the previous section's analysis, the failure mode under quasi-static conditions typically starts with interface debonding. When considering strain rate and temperature, Figure 6-14 shows that the crack propagation paths for loading velocities of 500 mm/s and 1000 mm/s are basically consistent, while at a loading velocity of 2000 mm/s, the crack path changes significantly. Additionally, it can be observed that as the loading velocity increases, the displacement at damage initiation also increases. These phenomena indicate that changes in strain rate affect the interfacial bonding strength and interfacial fracture energy, leading to differences in crack propagation paths. Furthermore, under a load velocity of 1000 mm/s, the influence of different initial temperatures was studied, and the numerical results are shown in Figure 10.

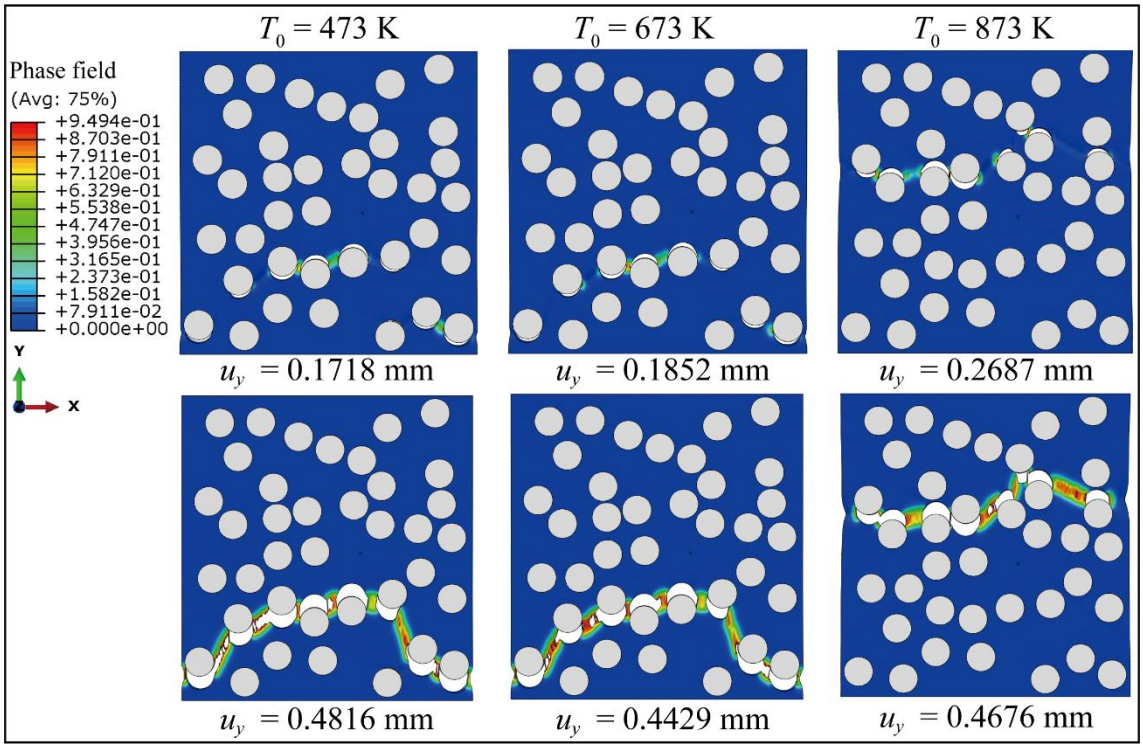

Figure 10 Crack propagation at different initial temperatures

Figure 10 shows that at initial temperatures T_0 = 473 K and 673 K, the crack initiation and propagation paths are basically the same. This means that at these two initial temperatures, the matrix still has relatively high strength, causing the interface to debond first. However, when the initial temperature rises to 873 K, the crack initiation and propagation path are no longer the same as in the previous two cases. Instead, debonding begins to occur at the interface in the central region of the RVE model, accompanied by the initiation of matrix cracks. This phenomenon indicates that as the initial temperature increases, the strength of the matrix gradually decreases, and the interfacial strength also decreases, but the extent of their decrease differs. This leads to the matrix strength and interfacial strength becoming comparable, resulting in changes in crack initiation and propagation paths. Further analysis suggests that if the initial temperature continues to increase, the matrix strength may fall below the interfacial strength, causing the matrix to crack first and the failure mode to transition from interface debonding to matrix cracking. Additionally, the influence of strain rate and temperature on the mechanical response of the multi-particle RVE model is shown in Figure 11.

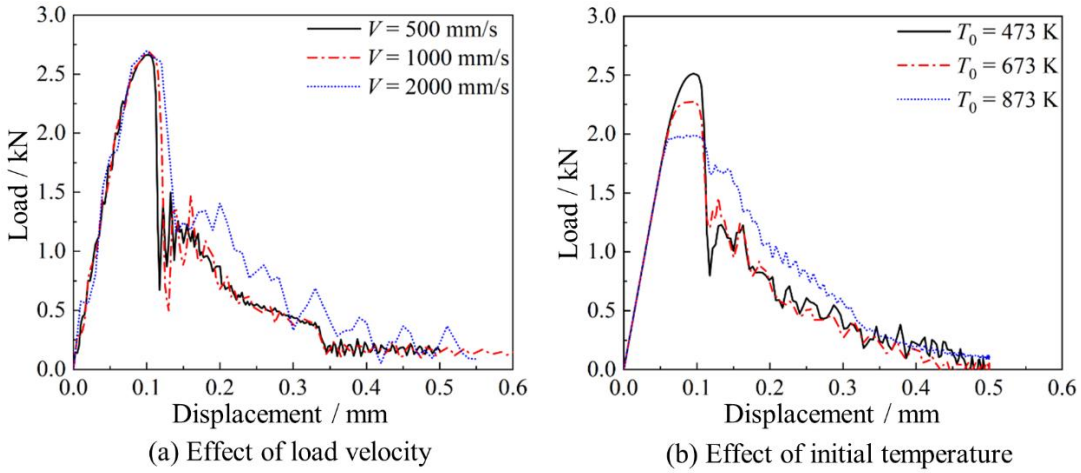

Figure 11 Influence of loading velocity and initial temperature on force-displacement curves

From Figure 11(a), it can be seen that as the loading velocity increases, the peak strength and failure displacement of the RVE model also increase, which is due to the consideration of the strain rate effect in the current model. The sudden drop in the load-displacement curve after reaching the peak strength indicates that multiple interfaces have debonded. Note that the displacement at interface failure in the load-displacement curve increases with loading velocity, indirectly illustrating the strengthening effect of strain rate on interfacial fracture energy. Furthermore, Figure11(b) shows that an increase in initial temperature leads to a decrease in peak strength, reflecting the softening effect of temperature. At T_0 = 473 K and 673 K, although the peak strength decreases, the failure displacements are relatively similar, indicating that under these conditions, the matrix material still maintains relatively high strength, and the failure mode remains dominated by interface debonding. When T_0 = 873 K, the latter part of the load-displacement curve shows an unusual increase in load instead of a decrease. This may be due to the significant softening of the matrix material at high temperature, making the interfacial strength comparable to the matrix strength, resulting in better bonding between the matrix and particles. In summary, the model in this chapter not only effectively characterizes the entire process from interface debonding to matrix cracking in the MMC RVE but also captures various failure mode changes under different strain rates and temperatures, providing a basis for composite structural optimization and failure analysis. Certainly, the validity of this model needs further verification through experiments in future work.

5. Summary

This study systematically investigated the failure behavior of Ti-6Al-4V/SiC composites at the mesoscale by coupling a ductile phase field model (PFM) with a cohesive zone model (CZM), revealing the failure mechanisms under the coupled effects of multiple factors such as interfacial strength, fracture energy, particle distribution, volume fraction, strain rate, and temperature. The results show that a smaller mesh size (0.05 mm) can more accurately capture matrix crack propagation; increasing interfacial strength and fracture energy significantly enhances the macroscopic mechanical properties of the composite; particle distribution affects local damage initiation, while increasing volume fraction improves stiffness and strength but reduces material ductility; strain rate strengthens interfacial fracture energy, while high temperature promotes a transition in failure mode from interface debonding to matrix-dominated cracking. The non-coupled CZM-PFM framework constructed in this study exhibits good numerical stability and physical realism, effectively simulating the complete failure process from interface debonding to matrix crack propagation. It provides a reliable numerical tool for multi-scale damage analysis and performance prediction of metal matrix composites.

However, the current model still has certain limitations: firstly, it does not consider the randomness of particle shape, size distribution, and interface properties; secondly, it is limited to a 2D model simplification and cannot fully reflect crack behavior under 3D stress states. Future work will focus on the following studies: First, experimental validation of interface failure behavior under different temperatures and strain rates to calibrate model parameters and improve prediction accuracy. Second, developing 3D multi-particle RVE models, incorporating random morphology and distribution characteristics to enhance the model's geometric realism. Further, extending the research to multi-field coupled loading conditions such as fatigue and creep to establish a more comprehensive failure analysis framework. Finally, combining machine learning

methods to optimize particle distribution and interface design, providing theoretical support and design tools for performance customization of composites.

Acknowledgments

This work has not received any funding support.

Conflicts of Interest

The authors declare that they have no known competing financial interests or personal relationships that could have appeared to influence the work reported in this paper.

References

References

[1] Nemat-Nasser, S., & Hori, M. (1993). Micromechanics: overall properties of heterogeneous materials. North-Holland.

[2] Needleman, A. (1987). A continuum model for void nucleation by inclusion debonding. Journal of Applied Mechanics, 54(3), 525-531.

[3] Tvergaard, V., & Hutchinson, J. W. (1992). The relation between crack growth resistance and fracture process parameters in elastic-plastic solids. Journal of the Mechanics and Physics of Solids, 40(6), 1377-1397.

[4] Ghosh, S., Lee, K., & Moorthy, S. (1995). Multiple scale analysis of heterogeneous elastic structures using homogenization theory and voronoi cell finite element method. International Journal of Solids and Structures, 32(1), 27-62.

[5] Vaughan, T. J., & McCarthy, C. T. (2011). A combined experimental--numerical approach for generating statistically equivalent fibre distributions for high strength laminated composite materials. Composites Science and Technology, 71(4), 577-598.

[6] Miehe, C., Welschinger, F., & Hofacker, M. (2010). Thermodynamically consistent phase-field models of fracture: Variational principles and multi-field FE implementations. International Journal for Numerical Methods in Engineering, 83(10), 1273-1311.

[7] Borden, M. J., Hughes, T. J., Landis, C. M., & Verhoosel, C. V. (2014). A higher-order phase-field model for brittle fracture: Formulation and analysis within the isogeometric analysis framework. Computer Methods in Applied Mechanics and Engineering, 273, 100-118.

[8] Li, T., Liu, Q., & Zhou, Z. (2019). A phase field model for simulating the fracture of composite materials with imperfect interfaces. Engineering Fracture Mechanics, 206, 25-44. [Cited as Ref. 227 in the text]

[9] Zhang, X., & Vignes, C. (2021). On the crack propagation behavior of brittle matrix composites: A comparative study using different strain energy decomposition methods in phase field models. Journal of the Mechanics and Physics of Solids, 147, 104252. [Cited as Ref. 228 in the text]

[10] Gurson, A. L. (1977). Continuum theory of ductile rupture by void nucleation and growth: Part I---Yield criteria and flow rules for porous ductile media. Journal of Engineering Materials and Technology, 99(1), 2-15.

[11] Eshelby, J. D. (1957). The determination of the elastic field of an ellipsoidal inclusion, and related problems. Proceedings of the Royal Society of London. Series A, Mathematical and Physical Sciences, 241(1226), 376-396.

[12] Mori, T., & Tanaka, K. (1973). Average stress in matrix and average elastic energy of materials with misfitting inclusions. Acta Metallurgica, 21(5), 571-574.